ACS APPLIED MATERIALS & INTERFACES

Research Article

Cite This: ACS Appl. Mater. Interfaces 2018, 10, 32426−32434

www.acsami.org

Influence of Systematic Incorporation of Conjugation-Break Spacers into Semi-Random Polymers on Mechanical and Electronic Properties

Elizabeth L. Melenbrink,[†] Kristan M. Hilby,[‡] Mohammad A. Alkhadra,[‡] Sanket Samal,[†] Darren J. Lipomi,*[,‡] and Barry C. Thompson*[,†]

[†]Department of Chemistry and Loker Hydrocarbon Research Institute, University of Southern California, Los Angeles, California 90089-1661, United States

[‡]Department of NanoEngineering, University of California, San Diego, 9500 Gilman Drive, Mail Code 0448, La Jolla, California 92093-0448, United States

Supporting Information

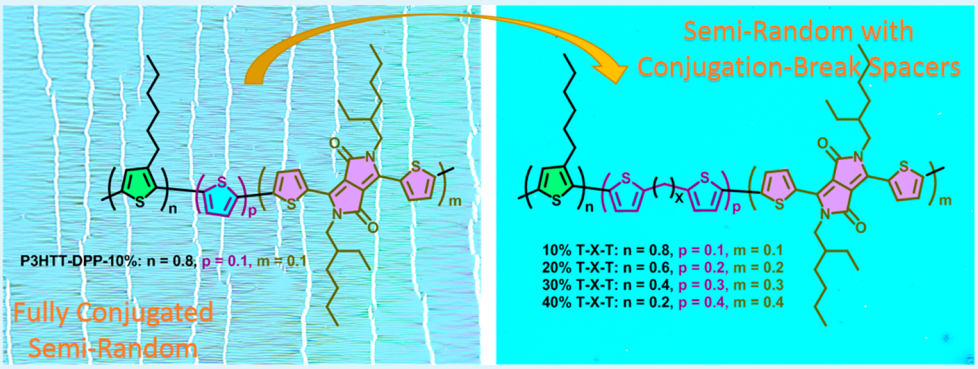

ABSTRACT: An extensive family of semi-random polymers was prepared via Stille polycondensation with varying contents of alkyl spacers incorporated into the polymer backbone to serve as a break in conjugation. This family was investigated to determine the effect of alkyl spacer length and percent incorporation on the optical, electronic, and mechanical properties. The optical bandgap was found to steadily increase from 1.53 to 1.70 eV as the amount of spacer was increased from 10 mol percent to 40 mol percent while the length of the spacer had little to no effect. In space charge limited current (SCLC) carrier mobility measurements, hole mobility was found to decrease as the amount of spacer increased but was found to steadily increase as the length of the spacer was increased from 6 to 10 carbons. Mechanical properties were observed by film-on-elastomer and film-on-water measurements, with low elastic moduli and high ductility attributed both to the break in conjugation as well as the semi-random structure of the polymer backbone. Measurements of the mechanical properties using the buckling method revealed elastic moduli between 0.14 and 1.3 GPa, and several polymers, when bonded to an elastomeric substrate, could be stretched beyond 80% strain. These polymers were further tested as free-standing films by obtaining a pull test on the surface of water, where we obtained tensile moduli between 0.13 and 0.75 GPa. These results indicate that semi-random polymers with conjugation-break spacers are promising candidates for further study in flexible electronics.

KEYWORDS: *conjugated polymers, conjugation-break spacer, semi-random polymers, mechanical properties, film-on-water*

INTRODUCTION

Organic electronic materials have been pursued for several decades with a vision of creating devices that are lightweight, flexible, and even stretchable to be suitable for a broad variety of applications. Conjugated polymers have many characteristics that make them attractive for these applications,[1] however, they tend to be brittle, inflexible, and have limited solubility and high melting points, making it impractical to incorporate them into industrial production. The rigid π-conjugated backbone of these materials, combined with the semicrystalline microstructure and the (often) glassy state of the amorphous domains at the operating temperature, has the effect of decreasing mechanical deformability and robustness. Different strategies have been pursued to try to overcome these mechanical and physical limitations, including side-chain engineering,[2,3] nanoconfinement,[4,5] blends with nonconjugated polymers,[6,7] and the creation of rod−coil-type block copolymers with conjugated and nonconjugated segments.[8,9] Many of these approaches dilute the electroactive component with insulating hydrocarbons, leading to a decrease in charge

Received: June 25, 2018
Accepted: September 4, 2018
Published: September 4, 2018

DOI: 10.1021/acsami.8b10608
ACS Appl. Mater. Interfaces 2018, 10, 32426−32434

Scheme 1. Semi-Random Polymers with Conjugation-Break Spacers Synthesized for This Study

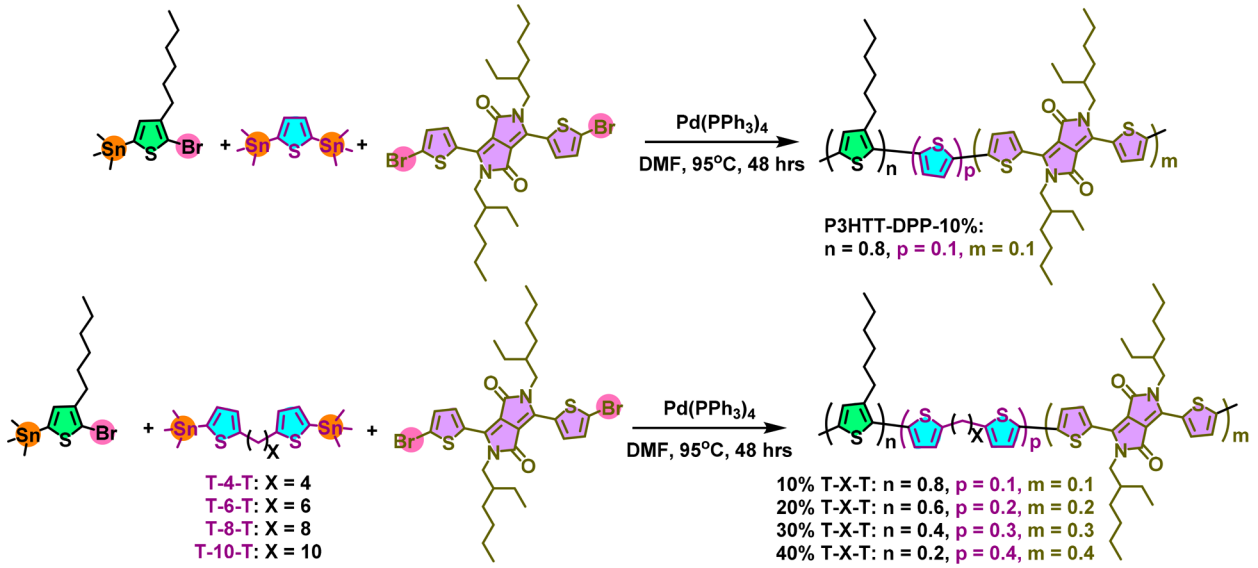

mobility. Additionally, several of these strategies require complex synthetic and processing conditions, increasing their ultimate cost. Thus, the desire arises to create simple, single-component semiconducting polymers with intrinsically robust mechanical properties.[10]

Over the past few years, a strategy from the 1990s[11−13] of incorporating nonconjugated segments into a conjugated polymer backbone has been revived with new versatility lent by improved polymerization techniques and a large library of electroactive monomers. An increasing number of groups have begun to study semiconducting polymers with a break in conjugation, seeking properties such as melt processability,[14] stretchability,[15] and even healable materials[16] by introducing additional modes for dissipation of mechanical energy (e.g., stretching of and rotation about aliphatic units).[17−21] The nonconjugated segments within the polymers are commonly known as conjugation-break spacers or CBSs. The Bao group has succeeded in making polymers that could almost fully recover their OFET charge mobility (1.13 vs 1.28 $cm^2 V^{-1} s^{-1}$) after healing a cut in the film by incorporating conjugation-break spacers capable of hydrogen bonding. The Mei group has synthesized a family of polymers with CBSs that so drastically lowered the polymer melting point (from 221 to 94 °C as spacer length increased) that it allowed for melt processing of thin films, eliminating the need for wasteful, toxic organic solvents. Previous work has suggested that mechanical properties such as the elastic modulus (E) depend on a complex interplay between molecular structure and packing arrangement in the solid state.[15] A lower elastic modulus is generally considered to be better for flexible electronics applications, as it indicates a material which is more easily deformed and which produces decreased interfacial stresses with other layers in a device. While elastic moduli of conjugated polymers vary widely (E = 0.1−8 GPa),[3,16,22−24] polymers with CBSs have consistently shown elastic moduli of less than 1 GPa.[15,16] However, they fall far short of conventional elastomers such as PDMS (E = 0.6−2.5 MPa)[25] or polyisoprene (E = 0.36 MPa).[26]

In previous examples of polymers containing CBS units, polymers were synthesized with a perfectly alternating or semi-alternating[27] (random) architecture, using AA and BB functionalized monomers.[21,28,29] The restricted linkage pattern in these polymers lends order to the polymer chain, which is propagated through the bulk and manifests itself in the high degree of crystallinity often seen in perfectly alternating polymers.[30,31] Herein, we introduce a semi-random architecture to polymers incorporating conjugation-break spacers, using AA, AB, and BB monomers. The less restrictive linkage pattern available to monomers in the semi-random polymer can increase disorder along the polymer backbone, a trait associated with decreased stiffness and brittleness in polymer films.[32,33] The semi-random architecture has also been shown to broaden the absorption of conjugated polymers over that of perfectly alternating polymers by creating a broader range of chromophores within the polymer backbone than is accessible with a perfectly alternating architecture.[34] Additionally, incorporating 3-hexylthiophene allows for the retention of the favorable properties of P3HT while tuning such properties as absorption, electronic energy levels, and surface energy.[35,36]

In this study, a family of semi-random polymers with conjugation-break spacers was synthesized via Stille polymerization (Scheme 1). CBSs were incorporated at 10%, 20%, 30%, and 40%, with spacer length varying between 4 and 10 methylene units. Due to the need to balance the AA/BB functional groups, the amount of the electron poor diketopyrrolopyrrole (DPP) acceptor monomer was increased at the same rate as the CBS, while simultaneously decreasing the amount of 3-hexylthiophene (3HT) monomer. Introducing randomness into the backbone of a conjugated polymer has been shown to decrease elastic modulus and increase crack-onset strain.[23] It was expected that the semi-random nature of the polymer backbones in this study would have a similar effect. The degrees of freedom added by conjugation-break spacers were expected to amplify these trends. As more methylene units were introduced into the spacer, we anticipated a decrease in elastic modulus (the ability of the material to resist deformation when a stress is applied to it) and ultimate tensile strength (UTS, the maximum stress that a material can withstand) due to the increased modes of dissipating mechanical energy excluding fracture.[37,38] In addition to probing the influence of structure on mechanical properties, we also aimed to expand our understanding of the

DOI: 10.1021/acsami.8b10608
ACS Appl. Mater. Interfaces 2018, 10, 32426−32434

Table 1. SEC, Thermal, and Electronic Data for Semi-Random Polymer Family

polymer	M_n[a] (kDa)	$Đ$[a]	T_m/T_c[b] (°C)	E_g[c] (eV)	HOMO[d] (eV)	μ_h[e] ($cm^2\ V^{-1}\ s^{-1}$)
P3HTT-DPP-10%	9.5	4.15	208/182	1.50	5.52	9.29×10^{-4}
10% T-4-T	10.5	4.30	-/-[f]	1.54	5.45	-[g]
10% T-6-T	29.0	4.79	-/-[f]	1.56	5.51	2.90×10^{-6}
10% T-8-T	19.7	6.23	-/-[f]	1.55	5.41	2.08×10^{-5}
10% T-10-T	14.0	3.68	-/-[f]	1.53	5.43	2.53×10^{-4}
20% T-4-T	8.4	4.90	-/-[f]	1.58	5.41	-[g]
20% T-6-T	17.6	4.28	-/-[f]	1.58	5.41	-[g]
20% T-8-T	14.2	5.15	-/-[f]	1.61	5.49	6.49×10^{-6}
20% T-10-T	12.4	5.24	-/-[f]	1.60	5.44	1.06×10^{-5}
30% T-4-T	6.4	2.87	-/-[f]	1.63	5.42	-[g]
30% T-6-T	14.4	5.42	-/-[f]	1.65	5.40	-[g]
30% T-8-T	9.9	5.15	90/81	1.66	5.43	-[g]
30% T-10-T	9.8	6.47	75/73	1.64	5.48	3.55×10^{-6}
40% T-4-T	7.4	2.90	-/-[f]	1.70	5.43	-[g]
40% T-6-T	10.5	5.09	143/112	1.68	5.41	-[g]
40% T-8-T	8.8	2.69	125/85	1.68	5.45	-[g]
40% T-10-T	12.2	2.98	83/76	1.68	5.50	-[h]

[a]Obtained via size-exclusion chromatography (SEC) versus polystyrene standards. [b]Obtained via differential scanning calorimetry (DSC). [c]Calculated from the absorption band edge in thin films, where $E_g = 1240/\lambda_{edge}$. [d]Estimated from cyclic voltammetry (CV) oxidation onset versus ferrocene. [e]Calculated from SCLC mobility measurements in hole-only devices with the architecture: ITO/PEDOT:PSS/polymer/Al, where the polymer layer was spin-cast from chloroform and annealed for 30 min at 150 °C prior to aluminum deposition. [f]No apparent thermal transitions. [g]Hole mobility not measured due to difficulty obtaining uniform films. [h]Not enough sample for annealed test; unannealed data in the Supporting Information.

scope of structure−function relationships in the versatile class of semi-random polymers.

RESULTS AND DISCUSSION

The family of 16 polymers with varying contents of CBS (and consequently DPP and 3HT monomers) and the fully conjugated reference polymer, P3HTT-DPP-10%, were synthesized via Stille polycondensation using methods previously developed in our group.[34] Solely even-numbered hydrocarbon chains were studied both for economic practicality and to eliminate a possible odd−even effect.[39] Polymers were named by the CBS monomer and the amount by which it was incorporated, e.g., 10% T-4-T indicates a CBS length of 4 carbons and that monomer makes up 10 mol percent of the polymer backbone, along with 10 mol percent of DPP and 80 mol percent 3HT. Polymer composition was confirmed by NMR to match the monomer feed ratios (Figures S2−S6). As increasing amounts of the alkyl spacers were incorporated into the polymer backbone, solubility in common halogenated solvents decreased, contrary to trends observed by Zhao et al.[21] Solubility is necessary not only for purifying and analyzing the polymers but also for processing them in their eventual use in organic electronics. The decrease in solubility was evidenced not only by increased difficulty with processing the polymers, particularly those with shorter spacers, but also the regular decrease in polymer molecular weight as the content of CBS increased (Table 1 and Table S1 and Figure S1). This could be due to the fact that DPP content was increased at the same rate as spacer content, with the poorly soluble acceptor monomer perhaps having a contradictory effect from that of the CBS. This effect diminished with the 10-carbon alkyl spacer. We suspect that the solubility-enhancing effects of the ten-carbon spacer outweighed the negative impact DPP had on solubility. Specifically, when 40% of the T-10-T monomer was incorporated into the polymer, a higher molecular weight was obtained than when only 30% of the ten-carbon spacer was used, contrary to the trend seen with every other spacer length. The entire T-10-T subfamily was easily soluble in chloroform at room temperature in contrast to the T-4-T subfamily. The polymer incorporating a four-carbon spacer at 40%, and thus DPP at 40%, required a chlorobenzene Soxhlet extraction to obtain a higher molecular weight (16.9 kDa) polymer fraction, but this fraction was not used for any subsequent analysis due to its poor solubility. These were generally high-yielding polymerizations, giving chloroform-soluble fractions at 60%−80% yield (Table S2).

The UV−vis spectra of the T-8-T subfamily are shown in Figure 1 as a representative example of optical trends. Spectra for all of the subfamilies are provided in Figures S7−S14. All polymers with a break in conjugation had a blue-shifted absorption onset, leading to a wider optical bandgap, when compared to the fully conjugated P3HTT-DPP-10% optical bandgap of 1.50 eV (Table 1). As the percentage of CBS and DPP incorporated into the polymer increased, the absorption onset continued to blue-shift to a maximum bandgap of 1.70 eV for the 40% T-X-T subfamily (Figure S15). Both of these trends are as expected, for the extended conjugation of a semiconducting polymer allows the highest occupied and lowest unoccupied molecular orbitals to draw nearer to each other, lowering the bandgap of the extended solid. By interrupting this extended sp^2 hybridization with the sp^3 hybridized carbons of alkyl chains, the bandgap increased and therefore the absorption onset moved to a higher energy. This is in contrast to a previous study from our group in which the absorption onset was found to red-shift and the bandgap to decrease with increasing DPP acceptor content in fully

DOI: 10.1021/acsami.8b10608
ACS Appl. Mater. Interfaces 2018, 10, 32426−32434

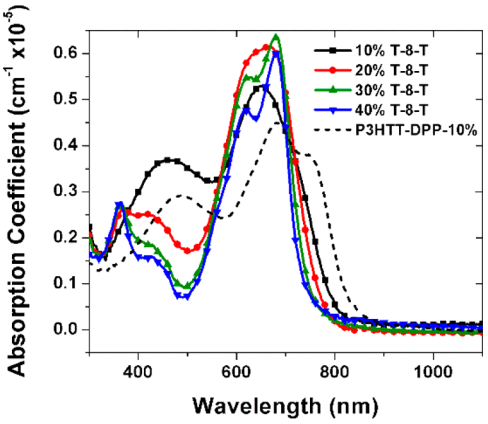

Figure 1. UV−vis absorption spectra of the T-8-T CBS subfamily thin films spin-cast from *o*-dichlorobenzene (o-DCB) and placed in a N_2 cabinet for 30 min. The P3HTT-DPP-10% absorption spectrum (dashed black line) is provided for a fully conjugated reference: (■) 10% T-8-T; (red ●) 20% T-8-T; (green ▲) 30% T-8-T; (blue ▼) 40% T-8-T.

conjugated semi-random polymers.[40] It is interesting to consider that perhaps the DPP and CBS monomers had contradictory effects on optical properties as well.

Only the percentage of conjugation-break spacer incorporated seemed to affect the absorption onset; the length of the CBS had no effect on the onset. However, experiments with different solvent and annealing conditions for the T-6-T subfamily indicated that there was a strong dependence of optical properties on processing conditions (Table S5 and Figure S16), which has been observed previously in semiconducting polymers.[41] From these experiments it is seen that both aromatic solvents and thermal annealing slightly increased the bandgap of the T-6-T polymers. As expected, absorption in the P3HT region of 400−550 nm decreased as CBS and acceptor content increased due to a consequent decrease in loading of the 3-hexylthiophene monomer (Figure 1).

Conjugated polymers are known for their high melting and crystallization temperatures, which were apparent in the fully conjugated P3HTT-DPP-10% polymer when analyzed by differential scanning calorimetry (DSC) (Figure S26). These thermal transitions can likely be attributed to crystallized P3HT segments present within the polymer, for P3HT has a melting point of 212 °C,[40] very close to the P3HTT-DPP-10% T_m of 208 °C. In contrast, no thermal transitions were observed in the semi-random polymers with lower incorporation of CBS, even though the 10% T-X-T subfamily has the same P3HT content as the fully conjugated P3HTT-DPP-10% polymer. This lack of thermal transitions is presumably due to the additional disorder contributed to the semi-random structure by the addition of the CBS. Melting and crystallization transitions became evident at higher percentages of CBS and DPP incorporation but only for longer spacers (e.g., 30% T-8-T, 30% T-10-T, 40% T-6-T, 40% T-8-T, and 40% T-10-T; see Tables S7 and S8 and Figures S32 and S33). The temperature of these thermal transitions decreased with increasing spacer length, as had been observed previously by Zhao et al.[39] This trend is attributable to a corresponding increase in polymer backbone flexibility, which lowered the melting and crystallization temperatures by increasing the entropy associated with those transitions.

An attempt to corroborate the DSC findings was made by observing crystallinity in thin films via grazing incidence X-ray diffraction (GIXRD). However, contrary to the findings above, within the CBS polymers, peaks were visible primarily for the 10% T-X-T subfamily (Figure S34 and Table S9). This is attributable to the high P3HT content in that family, as the 100 diffraction peak in P3HT corresponds to a lamellar packing distance of 16.7 Å,[42] which nearly matches the average distance of 16.3 Å for the 10% T-X-T subfamily. The fully conjugated, semicrystalline P3HTT-DPP-10% polymer packed closer at 15.7 Å, as previously observed.[35] Interestingly, the intensity of the diffraction peak decreased steadily as the spacer length increased across the 10% T-X-T subfamily, with the exception of 10% T-10-T, which showed a sharp increase, exhibiting even more crystallinity than the fully conjugated P3HTT-DPP-10% polymer. It could be that when the spacer reached ten methylene units in length, it had sufficient flexibility to allow better intra- and intermolecular packing, leading to a more intense diffraction peak. This improved packing could also explain why the 20% T-10-T polymer was the only one in the 20% T-X-T subfamily to exhibit a diffraction peak. The 20% T-10-T peak was likely much less intense than its 10% T-10-T cousin due to the 20% decrease in 3HT monomer content between the two, though it appeared to have approximately the same lamellar packing distance (16.0 Å). A small diffraction peak was observed in the same region for the 40% T-6-T polymer, but it was not distinct enough to obtain a Gaussian fit.

The highest occupied molecular orbital (HOMO) energy was calculated from oxidation onset using cyclic voltammetry (CV). As can be seen in Table 1 (and Figure S25), there were no observable trends in the HOMOs of these polymers. All values were approximately the same, producing an average HOMO of 5.44 ± 0.04 eV (within the instrument error of ±0.05 eV). This was slightly more shallow than the 5.52 eV HOMO of the fully conjugated P3HTT-DPP-10%. This trend (or lack thereof) closely matches that seen by Zhao et al., where they observed no effect on the HOMO from increasing the CBS length.[39] However, in their study, the polymers were perfectly alternating between DPP and spacer monomers, maintaining the same electroactive moiety regardless of spacer length. Therefore, there was no change in the effective conjugation length as spacer length was varied, which would lead one to assume that there would be no change in frontier orbital energy levels. In contrast, in this study, the amount of spacer as well as its potential distribution within the polymer was varied, which makes the consistent HOMO energy more surprising.

To determine if the spacer length and content influenced charge mobility, SCLC measurements were performed on hole-only devices. However, due to the poor solubility of some of the polymers and the resulting difficulty in obtaining uniform films, only 8 of the 17 polymers were measured (Table 1 and Tables S10−S13). Annealed films spin-cast from chloroform are presented herein; films cast from *ortho*-dichlorobenzene showed no trends and are presented in the Supporting Information (Table S11), along with as-cast films from chloroform (Tables S10 and S12 and Figure S35). From the data points obtained, it can be seen that mobility decreased as the content of spacer increased in the T-10-T subfamily. This correlates with observations made in the literature for mobility values decreasing as spacer content increased due to a larger amount of insulating alkyl chains interrupting charge

DOI: 10.1021/acsami.8b10608
ACS Appl. Mater. Interfaces 2018, 10, 32426−32434

transport along the polymer backbone.[21] However, a counterintuitive trend emerged within the 10% T-X-T (and, to a lesser extent, the 20% T-X-T) subfamily. In these measurements, the hole mobility appeared to increase as the length of the CBS increased, contrary to trends observed by Zhao et al.[39] This is counterintuitive because the polymers with longer spacers have more insulating hydrocarbon units per mole than those with shorter CBSs. However, we reason that the longer spacers possibly gave the polymer increased flexibility and more easily allowed the electroactive portions of the polymer chain to rearrange and stack themselves in a manner favorable for charge transport. This corresponds well with the highest charge mobility coming from the 10% T-10-T polymer (2.53×10^{-4} cm^2 V^{-1} s^{-1}), which also had the most intense diffraction peak, indicating higher crystallinity due to improved packing. Remarkably, this value for hole mobility is the same order of magnitude as that obtained for the fully conjugated P3HTT-DPP-10% analogue (9.29×10^{-4} cm^2 V^{-1} s^{-1}), signifying that a 10% incorporation of conjugation-break spacer did not greatly impede charge mobility.

To test our hypothesis about semi-random CBS incorporation contributing to improved mechanical properties, film-on-elastomer mechanical tests were performed on the entire family of 16 polymers as well as the fully conjugated P3HTT-DPP-10% polymer. Several interesting trends were observed (Table 2 and Table S14 and Figure S45). The elastic (Young's) modulus, E, is the ratio of stress σ, or force per cross sectional area of a deformed body, to strain ε, or fractional amount of deformation in the direction of applied force, in the linear region of a stress−strain curve.[1] The modulus is a quantitative measure of the ability of a material to store mechanical energy reversibly or its elasticity. This property is strongly related to the solid-state morphology, as well as the molecular structure, of the material.[15] The more closely polymer chains can pack, the greater the density of load-bearing carbon−carbon bonds along the strained axis and the greater the intermolecular forces between chains. As aforementioned, a lower elastic modulus is generally considered to be favorable for applications involving flexible electronics, as it corresponds to a more compliant material. The elastic modulus in our polymers increased when the spacer content was increased from 10% to 20% incorporation for all spacer lengths and most of the 40% T-X-T subfamily were unattainable due to poor film-forming ability. It is noteworthy that the elastic modulus of 0.32 GPa for the fully conjugated semi-random P3HTT-DPP-10% polymer is itself in the lower range of moduli observed in perfectly alternating fully conjugated polymers.[16,22,23,43] It is interesting that the 10% CBS subfamily exhibited improved elastic moduli compared to the fully conjugated analogue, but this trend was reversed for the 20% CBS subfamily. This could be due to the aforementioned contradictory effect introduced by increasing the ratio of the stiff DPP monomer along with the flexible CBS monomer. With the exception of 20% T-4-T, this entire polymer family fit the trend of CBS polymers consistently displaying elastic moduli <1 GPa.

Table 2. Mechanical Properties Obtained from Film-on-Elastomer Measurements for Semi-Random Polymer Family

polymer	elastic modulus (GPa)[a]	crack-onset strain (%)[b]	mode of failure[b]
P3HTT-DPP-10%	0.32 ± 0.20	10	brittle
10% T-4-T	0.33 ± 0.11	27	ductile
10% T-6-T	0.15 ± 0.02	>80[c]	ductile
10% T-8-T	0.14 ± 0.06	>80[c]	ductile
10% T-10-T	0.15 ± 0.04	>80[c]	ductile
20% T-4-T	1.30 ± 0.42	2	brittle
20% T-6-T	0.51 ± 0.16	37	ductile
20% T-8-T	0.65 ± 0.32	>80[c]	ductile
20% T-10-T	0.52 ± 0.12	>80[c]	ductile
30% T-4-T	0.15 ± 0.09	<1	brittle
30% T-6-T	-[d]	-[d]	-[d]
30% T-8-T	0.59 ± 0.15	<1	brittle
30% T-10-T	0.60 ± 0.07	>80[c]	ductile
40% T-4-T	-[d]	1	brittle
40% T-6-T	-[d]	-[d]	-[d]
40% T-8-T	-[d]	1	brittle
40% T-10-T	0.60 ± 0.30	77	ductile

[a]Calculated using the buckling-based metrology and averaged over three measurements. [b]Obtained from optical micrographs. [c]Test terminated at 80% strain due to potential for PDMS substrate breakage. [d]Data unattainable due to inability to form uniform films.

Crack-onset strain (COS) or the strain at failure (when cracks first appear in the polymer film) was also obtained from film-on-elastomer measurements. This value is a direct measurement of film ductility and provides important insight about film stretchability.[10,44] There were clear trends both in the COS and mode of failure as spacer length and percent incorporation increased (Table 2, Table S15, Figure S46, and Table S17). Ductile films failed by forming pinholes (Figure S48), while brittle films failed by forming parallel, slender cracks (Figure S47). All of the 10% T-X-T subfamily and the entire T-10-T subfamily exhibited ductile behavior, while the higher incorporation of CBS and shorter spacers exhibited brittle behavior. This correlated with the COS increasing as the alkyl spacer became longer and decreasing as more CBS was incorporated into the polymer chain. Again, the general decrease in ductility with increasing CBS incorporation is attributed not to the alkyl spacer itself, which was expected to improve mechanical properties, but to the corresponding increase in DPP monomer incorporation. Notably, the COS of 10% for the fully conjugated P3HTT-DPP-10% polymer is at the higher end of the range typically observed for fully conjugated perfectly alternating polymers.[15,16,22] This is attributable to the more randomized monomer distribution along the backbone attainable with semi-random polymers, leading to decreased order.[45] It should be noted that several of the COS values obtained for this polymer family are extraordinarily high (>80%). In measuring COS, we terminated the film-on-elastomer tensile test beyond 80% applied strain due to breakage of the PDMS substrate. For this reason, further measurements of free-standing films were pursued using an alternative technique for the seven polymers exhibiting a COS near or greater than 80%.

The mechanical properties of the seven polymers were further investigated using a method originally developed by Kim and co-workers, where a tensile test is performed on a film supported by water (Figure 2).[46] This "film-on-water" technique is a modified version of a conventional pull test (which involves suspending the specimen in air). The film is able to float and slide unimpeded on the surface due to the

DOI: 10.1021/acsami.8b10608
ACS Appl. Mater. Interfaces 2018, 10, 32426−32434

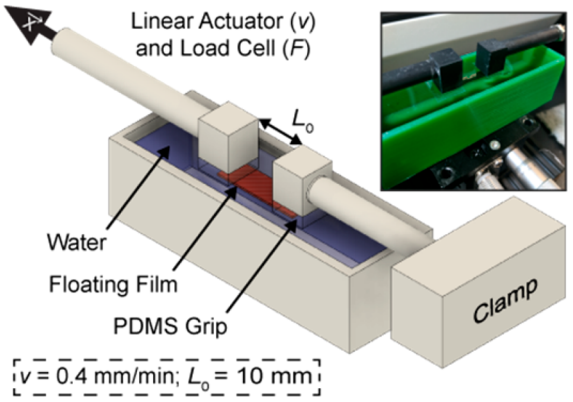

Figure 2. Pseudo free-standing tensile test of P3HT-based semi-random copolymers. Schematic representation of experimental setup, which includes a floating film, linear actuator, load cell, and trough filled with water. Inset photograph demonstrates the real experimental apparatus.

high surface tension and low viscosity of water. The mechanical properties obtained by this method can be considered a "definitive" measurement of the inherent polymer properties, whereas those obtained through film-on-elastomer measurements are a more realistic approximation of mechanical behavior in devices.[47] Stress−strain curves acquired for this study were produced by transforming the obtained curves of force versus displacement using the dimensions of the corresponding sample. From these curves were obtained the elastic modulus, toughness, ultimate tensile strength (UTS), and fracture strength, with the results tabulated in Table 3.

Table 3. Tabulated Values of Mechanical Properties Using the Film-on-Water Technique

polymer	modulus (GPa)[a]	toughness (MPa)[b]	UTS (MPa)[c]	fracture strength (MPa)[d]
10% T-6-T	0.23 ± 0.03	1.4 ± 0.3	7.8 ± 0.7	7 ± 1
10% T-8-T	0.14 ± 0.03	1.5 ± 0.5	6.9 ± 0.9	6.6 ± 0.5
10% T-10-T	0.13 ± 0.01	1.0 ± 0.5	5 ± 1	5 ± 1
20% T-8-T	0.42 ± 0.03	2.6 ± 0.4	13 ± 1	13 ± 1
20% T-10-T	0.32 ± 0.03	1.8 ± 0.2	8.6 ± 0.4	7 ± 2
30% T-10-T	0.33 ± 0.04	2 ± 1	11 ± 1	10 ± 1
40% T-10-T	0.75 ± 0.08	1.9 ± 0.4	19.3 ± 0.4	16 ± 3

[a]Elastic moduli can be derived from stress−strain curves by taking the slope of the linear regime of the graph. [b]Toughness values are obtained by integrating the entirety of the stress−strain curve. [c]UTS is obtained from the maximum stress in the stress−strain curve. [d]Fracture strength is obtained from a stress−strain curve by reading the stress at failure.

Toughness is the amount of energy per unit volume that a material will absorb before fracturing. Since toughness is dependent on the area under the stress−strain curve, an increase in strength or extensibility of the material will improve the toughness of the material. There is also a general trend suggesting that greater intermolecular forces between polymer chains will improve the toughness.[1] UTS reflects the maximum stress that the material withstands prior to fracture, and fracture strength is the stress at which the material fractures. The extensibility, or the fracture strain, is the strain at which the material fractures. Sometimes this quantity is called the "stretchability," though we do not generally support the use of this word when referring to mechanical properties because it has different meanings to different communities.[48]

Trends within the film-on-water data are plotted in Figure 3, where **3a−3c** show the effects of spacer length and **3d−3f** demonstrate the effects of spacer content on mechanical properties. Increasing the number of sp^3 bonds in the backbone of the polymer increases the ability of the bonds along the polymer chains to rotate; we therefore predicted that incorporation of conjugation-break spacers within the backbone would increase the ability of a solid material to be deformed. Indeed, we observed a decrease in elastic modulus and UTS as spacer length increased (Figure 3b,c) and a relatively small effect on toughness (**3b**). These measurements allowed us to distinguish the mechanical properties between 10% T-6-T, 10% T-8-T, and 10% T-10-T, which had nearly identical behavior when measured using film-on-elastomer techniques. Figure 3d shows the effect of the fraction of the spacer and the DPP unit on the mechanical properties. The most striking feature of the stress−strain behavior is the increase in stress and decrease in extensibility with increasing fraction of the spacer and the DPP unit, again perhaps attributable to the contradictory effects of simultaneously increasing CBS and DPP content. The modulus also increased, as shown in Figure 3e. Toughness, as plotted in Figure 3e, is a function of both the stress and the extensibility, so though it appears that there was little change in toughness among the polymers with varied T-10-T content, their underlying stress and extensibility properties were quite different. It is worth noting that the fraction of the spacer and DPP segments seemed to have more significant effects on the mechanical properties of the materials than the spacer length.

In short, modulating the length and fraction of the spacer in these low-bandgap conjugated polymers had a strong effect on the deformability. Introducing more carbon atoms into the spacer generally had the effect of decreasing the elastic modulus, toughness, and UTS. Increasing the fraction of the conjugation-break spacer and the DPP unit increased the values of these properties, making the material stronger, but also less extensible. Overall, the effects from modulating the fraction of the spacer and DPP monomers were more significant than the modulation of the length of the spacer. Although the samples tested varied in molecular weight, trends were still observed despite the fact that mechanical properties have been shown to depend strongly on molecular weight in homopolymers.[49]

CONCLUSIONS

In summary, a family of semi-random polymers with conjugation-break spacers was synthesized exhibiting notable mechanical properties, attributed both to the break in conjugation as well as the semi-random structure of the polymer backbone. Film-on-elastomer measurements revealed low elastic moduli between 0.14 and 1.3 GPa and several polymers could be stretched beyond 80% strain before film failure. Further testing of these polymers as free-standing films using film-on-water methods confirmed low elastic moduli between 0.13 and 0.75 GPa. While the electronic properties are generally diminished relative to similar semiconducting polymers, the trends observed in optical bandgap and hole mobility suggest that these properties could be tuned and

DOI: 10.1021/acsami.8b10608
ACS Appl. Mater. Interfaces 2018, 10, 32426−32434

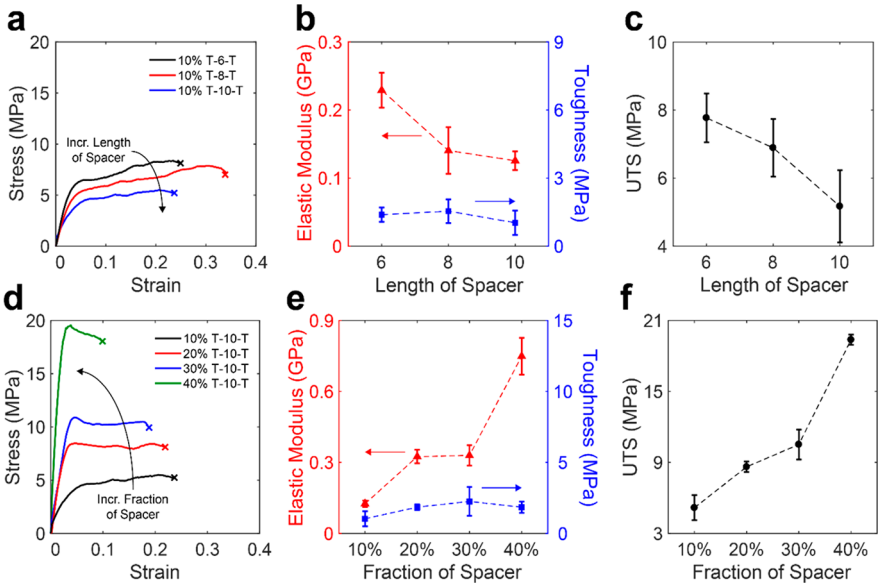

Figure 3. Stress–strain curves and corresponding mechanical properties as functions of the length (with 10% incorporation of the spacer) and fraction of the aliphatic spacer (with 10 carbon atoms in the spacer). (a,d) Representative stress–strain curves of pristine films obtained using the film-on-water technique. Correlation of toughness and elastic modulus with (b) the length and (e) the fraction of the spacer. Values of toughness are obtained by integrating the total area under the stress–strain curves. Values of elastic modulus are calculated as the slope of the linear region of the graph. Relationship between ultimate tensile strength (UTS) and (c) the length or (f) the fraction of the spacer. UTS values were obtained from the stress–strain curves from the stress at fracture. Mean values and error bars (standard deviations based on 95% confidence bounds) are based on data collected from at least three separate measurements. Dashed lines are to guide the eyes.

optimized in the future. In fact, the 10% T-10-T polymer seems to be a promising starting point for future optimization, with its high mobility of 2.53×10^{-4} cm^2 V^{-1} s^{-1}, which is comparable to the fully conjugated P3HTT-DPP-10% mobility of 9.29×10^{-4} cm^2 V^{-1} s^{-1}. This ductile polymer had the lowest elastic modulus as measured by both film-on-water and film-on-elastomer techniques, and film-on-elastomer measurements revealed a crack-onset strain of greater than 80%. These results indicate that semi-random polymers with conjugation-break spacers are promising candidates for further study in flexible electronics. In future studies, we plan to elucidate the effects of increasing the CBS without increasing the DPP content, as there were several measurements wherein the two monomers appeared to have contradictory effects. We also plan to clarify the effects of limited solubility on the measurements by lengthening the DPP side chain.

■ ASSOCIATED CONTENT

Supporting Information

The Supporting Information is available free of charge on the ACS Publications website at DOI: 10.1021/acsami.8b10608.

Additional materials and methods, synthetic data, and characterization data and spectra (PDF)

■ AUTHOR INFORMATION

Corresponding Authors

*E-mail: barrycth@usc.edu.
*E-mail: dlipomi@eng.ucsd.edu.

ORCID

Darren J. Lipomi: 0000-0002-5808-7765
Barry C. Thompson: 0000-0002-3127-0412

Author Contributions

The manuscript was written through contributions of all authors. All authors have given approval to the final version of the manuscript.

Notes

The authors declare no competing financial interest.

■ ACKNOWLEDGMENTS

B.C.T. acknowledges support by the National Science Foundation (CBET Energy for Sustainability) Grant CBET-1436875. D.J.L. acknowledges support from the Air Force Office of Scientific Research Grant FA9550-16-1-0220.

■ REFERENCES

(1) Root, S. E.; Savagatrup, S.; Printz, A. D.; Rodriquez, D.; Lipomi, D. J. Mechanical Properties of Organic Semiconductors for Stretchable, Highly Flexible, and Mechanically Robust Electronics. *Chem. Rev.* **2017**, *117*, 6467–6499.

(2) Wu, H.; Hung, C.; Hong, C.; Sun, H.; Wang, J.; Yamashita, G.; Higashihara, T.; Chen, W. Isoindigo-Based Semiconducting Polymers using Carbosilane Side Chains for High Performance Stretchable Field-Effect Transistors. *Macromolecules* **2016**, *49*, 8540–8548.

(3) Savagatrup, S.; Makaram, A. S.; Burke, D. J.; Lipomi, D. J. Mechanical Properties of Conjugated Polymers and Polymer-Fullerene Composites as a Function of Molecular Structure. *Adv. Funct. Mater.* **2014**, *24*, 1169–1181.

(4) Xu, J.; Wang, S.; Wang, G. N.; Zhu, C.; Luo, S.; Jin, L.; Gu, X.; Chen, S.; Feig, V. R.; To, J. W. F.; Rondeau-Gagné, S.; Park, J.; Schroeder, B. C.; Lu, C.; Oh, J. Y.; Wang, Y.; Kim, Y.; Yan, H.; Sinclair, R.; Zhou, D.; Xue, G.; Murmann, B.; Linder, C.; Cai, W.; Tok, J. B. H.; Chung, J. W.; Bao, Z. Highly Stretchable Polymer Semiconductor Films through the Nanoconfinement Effect. *Science* **2017**, *355*, 59–64.

(5) Shin, M.; Oh, J. Y.; Byun, K.; Lee, Y.; Kim, B.; Baik, H.; Park, J.; Jeong, U. Polythiophene Nanofibril Bundles Surface-Embedded in

DOI: 10.1021/acsami.8b10608
ACS Appl. Mater. Interfaces 2018, 10, 32426–32434

Elastomer: A Route to a Highly Stretchable Active Channel Layer. *Adv. Mater.* **2015**, *27*, 1255−1261.
(6) Ocheje, M. U.; Charron, B. P.; Nyayachavadi, A.; Rondeau-Gagné, S. Stretchable Electronics: Recent Progress in the Preparation of Stretchable and Self-Healing Semiconducting Conjugated Polymers. *Flexible Printed Electron.* **2017**, *2*, 043002.
(7) Taroni, P. J.; Santagiuliana, G.; Wan, K.; Calado, P.; Qiu, M.; Zhang, H.; Pugno, N. M.; Palma, M.; Stingelin-Stutzman, N.; Heeney, M.; Fenwick, O.; Baxendale, M.; Bilotti, E. Toward Stretchable Self-Powered Sensors Based on the Thermoelectric Response of PEDOT:PSS/Polyurethane Blends. *Adv. Funct. Mater.* **2018**, *28*, 1704285.
(8) Müller, C. C.; Goffri, S.; Breiby, D. W.; Andreasen, J. W.; Chanzy, H. D.; Janssen, R. R.; Nielsen, M.; Radano, C. P. C.; Sirringhaus, H.; Smith, P. P.; Stutzmann, N. Tough, Semiconducting Polyethylene-Poly(3-Hexylthiophene) Diblock Copolymers. *Adv. Funct. Mater.* **2007**, *17*, 2674−2679.
(9) Kim, H. J.; Kim, J.; Ryu, J.; Kim, Y.; Kang, H.; Lee, W. B.; Kim, T.; Kim, B. J. Architectural Engineering of Rod-Coil Compatibilizers for Producing Mechanically and Thermally Stable Polymer Solar Cells. *ACS Nano* **2014**, *8*, 10461−10470.
(10) Savagatrup, S.; Printz, A. D.; O'Connor, T. F.; Zaretski, A. V.; Lipomi, D. J. Molecularly Stretchable Electronics. *Chem. Mater.* **2014**, *26*, 3028−3041.
(11) Hong, Y.; Miller, L. L. An Electrically Conducting Polyester that has Isolated Quatrathiophene Units in the Main Chain. *Chem. Mater.* **1995**, *7*, 1999−2000.
(12) Kunugi, Y.; Miller, L. L.; Maki, T.; Canavesi, A. Photodiodes Utilizing Polyesters that Contain Different Colored Oligothiophenes in the Main Chain. *Chem. Mater.* **1997**, *9*, 1061−1062.
(13) Donat-Bouillud, A.; Mazerolle, L.; Gagnon, P.; Goldenberg, L.; Petty, M. C.; Leclerc, M. Synthesis, Characterization, and Processing of New Electroactive and Photoactive Polyesters Derived from Oligothiophenes. *Chem. Mater.* **1997**, *9*, 2815−2821.
(14) Zhao, Y.; Zhao, X.; Roders, M.; Gumyusenge, A.; Ayzner, A. L.; Mei, J. Melt-Processing of Complementary Semiconducting Polymer Blends for High Performance Organic Transistors. *Adv. Mater.* **2017**, *29*, 1605056.
(15) Savagatrup, S.; Zhao, X.; Chan, E.; Mei, J.; Lipomi, D. J. Effect of Broken Conjugation on the Stretchability of Semiconducting Polymers. *Macromol. Rapid Commun.* **2016**, *37*, 1623−1628.
(16) Oh, J. Y.; Rondeau-Gagné, S.; Chiu, Y.; Chortos, A.; Lissel, F.; Wang, G. N.; Schroeder, B. C.; Kurosawa, T.; Lopez, J.; Katsumata, T.; Xu, J.; Zhu, C.; Gu, X.; Bae, W.; Kim, Y.; Jin, L.; Chung, J. W.; Tok, J. B. -.; Bao, Z. Intrinsically Stretchable and Healable Semiconducting Polymer for Organic Transistors. *Nature* **2016**, *539*, 411−415.
(17) Gasperini, A.; Bivaud, S.; Sivula, K. Controlling Conjugated Polymer Morphology and Charge Carrier Transport with a Flexible-Linker Approach. *Chem. Sci.* **2014**, *5*, 4922−4927.
(18) Wijsboom, Y. H.; Patra, A.; Zade, S. S.; Sheynin, Y.; Li, M.; Shimon, L. J. W.; Bendikov, M. Controlling Rigidity and Planarity in Conjugated Polymers: Poly(3,4-Ethylenedithioselenophene). *Angew. Chem., Int. Ed.* **2009**, *48*, 5443−5447.
(19) Ong, B. S.; Wu, Y.; Liu, P.; Gardner, S. High-Performance Semiconducting Polythiophenes for Organic Thin-Film Transistors. *J. Am. Chem. Soc.* **2004**, *126*, 3378−3379.
(20) McCulloch, I.; Heeney, M.; Bailey, C.; Genevicius, K.; MacDonald, I.; Shkunov, M.; Sparrowe, D.; Tierney, S.; Wagner, R.; Zhang, W.; Chabinyc, M. L.; Kline, R. J.; McGehee, M.D.; Toney, M. F. Liquid-Crystalline Semiconducting Polymers with High Charge-Carrier Mobility. *Nat. Mater.* **2006**, *5*, 328−333.
(21) Zhao, Y.; Zhao, X.; Zang, Y.; Di, C.; Diao, Y.; Mei, J. Conjugation-Break Spacers in Semiconducting Polymers: Impact on Polymer Processability and Charge Transport Properties. *Macromolecules* **2015**, *48*, 2048−2053.
(22) Roth, B.; Savagatrup, S.; de los Santos, N. V.; Hagemann, O.; Carlé, J. E.; Helgesen, M.; Livi, F.; Bundgaard, E.; Søndergaard, R. R.; Krebs, F. C.; Lipomi, D. J. Mechanical Properties of a Library of Low-Band-Gap Polymers. *Chem. Mater.* **2016**, *28*, 2363−2373.
(23) Printz, A. D.; Savagatrup, S.; Burke, D. J.; Purdy, T. N.; Lipomi, D. J. Increased Elasticity of a Low-Bandgap Conjugated Copolymer by Random Segmentation for Mechanically Robust Solar Cells. *RSC Adv.* **2014**, *4*, 13635−13643.
(24) Zhou, J.; Li, E. Q.; Li, R.; Xu, X.; Ventura, I. A.; Moussawi, A.; Anjum, D. H.; Hedhili, M. N.; Smilgies, D.; Lubineau, G.; Thoroddsen, S. T. Semi-Metallic, Strong and Stretchable Wet-Spun Conjugated Polymer Microfibers. *J. Mater. Chem. C* **2015**, *3*, 2528−2538.
(25) Khanafer, K.; Duprey, A.; Schlicht, M.; Berguer, R. Effects of Strain Rate, Mixing Ratio, and Stress−strain Definition on the Mechanical Behavior of the Polydimethylsiloxane (PDMS) Material as Related to its Biological Applications. *Biomed. Microdevices* **2009**, *11*, 503−508.
(26) Baboo, M.; Dixit, M.; Sharma, K.; Saxena, N. Mechanical and Thermal Characterization of Cis-Polyisoprene and Trans-Polyisoprene Blends. *Polym. Bull.* **2011**, *66*, 661−672.
(27) Howard, J. B.; Thompson, B. C. Design of Random and Semi-Random Conjugated Polymers for Organic Solar Cells. *Macromol. Chem. Phys.* **2017**, *218*, 1700255.
(28) Schroeder, B. C.; Chiu, Y.; Gu, X.; Zhou, Y.; Xu, J.; Lopez, J.; Lu, C.; Toney, M. F.; Bao, Z. Non-Conjugated Flexible Linkers in Semiconducting Polymers: A Pathway to Improved Processability without Compromising Device Performance. *Adv. Electron. Mater.* **2016**, *2*, 1600104.
(29) Li, H.; Wang, J.; Mei, C.; Li, W. A New Class of Organic Photovoltaic Materials: Poly(Rod-Coil) Polymers having Alternative Conjugated and Non-Conjugated Segments. *Chem. Commun.* **2014**, *50*, 7720−7722.
(30) Thompson, B. C.; Kim, B. J.; Kavulak, D. F.; Sivula, K.; Mauldin, C.; Fréchet, J. M. J. Influence of Alkyl Substitution Pattern in Thiophene Copolymers on Composite Fullerene Solar Cell Performance. *Macromolecules* **2007**, *40*, 7425−7428.
(31) Noriega, R.; Rivnay, J.; Vandewal, K.; Koch, F. P. V.; Stingelin, N.; Smith, P.; Toney, M. F.; Salleo, A. A General Relationship between Disorder, Aggregation and Charge Transport in Conjugated Polymers. *Nat. Mater.* **2013**, *12*, 1038−1044.
(32) O'Connor, B.; Chan, E. P.; Chan, C.; Conrad, B. R.; Richter, L. J.; Kline, R. J.; Heeney, M.; McCulloch, I.; Soles, C. L.; DeLongchamp, D. M. Correlations between Mechanical and Electrical Properties of Polythiophenes. *ACS Nano* **2010**, *4*, 7538−7544.
(33) Awartani, O.; Lemanski, B. I.; Ro, H. W.; Richter, L. J.; DeLongchamp, D. M.; O'Connor, B. T. Correlating Stiffness, Ductility, and Morphology of Polymer:Fullerene Films for Solar Cell Applications. *Adv. Energy Mater.* **2013**, *3*, 399−406.
(34) Burkhart, B.; Khlyabich, P. P.; Cakir Canak, T.; LaJoie, T. W.; Thompson, B. C. Semi-Random" Multichromophoric rr-P3HT Analogues for Solar Photon Harvesting. *Macromolecules* **2011**, *44*, 1242−1246.
(35) Khlyabich, P. P.; Burkhart, B.; Ng, C. F.; Thompson, B. C. Efficient Solar Cells from Semi-Random P3HT Analogues Incorporating Diketopyrrolopyrrole. *Macromolecules* **2011**, *44*, 5079−5084.
(36) Howard, J. B.; Ekiz, S.; Noh, S.; Thompson, B. C. Surface Energy Modification of Semi-Random P3HTT-DPP. *ACS Macro Lett.* **2016**, *5*, 977−981.
(37) Rabinovich, A. L.; Ripatti, P. O. The Flexibility of Natural Hydrocarbon Chains with Non-Methylene-Interrupted Double Bonds. *Chem. Phys. Lipids* **1991**, *58*, 185−192.
(38) Rey, A.; Kolinski, A.; Skolnick, J.; Levine, Y. K. Effect of Double Bonds on the Dynamics of Hydrocarbon Chains. *J. Chem. Phys.* **1992**, *97*, 1240−1249.
(39) Zhao, X.; Zhao, Y.; Ge, Q.; Butrouna, K.; Diao, Y.; Graham, K. R.; Mei, J. Complementary Semiconducting Polymer Blends: The Influence of Conjugation-Break Spacer Length in Matrix Polymers. *Macromolecules* **2016**, *49*, 2601−2608.

DOI: 10.1021/acsami.8b10608
ACS Appl. Mater. Interfaces 2018, 10, 32426−32434

(40) Ekiz, S.; Gobalasingham, N. S.; Thompson, B. C. Exploring the Influence of Acceptor Content on Semi-random Conjugated Polymers. *J. Polym. Sci., Part A: Polym. Chem.* **2017**, *55*, 3884−3892.
(41) Kline, R. J.; McGehee, M. D.; Kadnikova, E. N.; Liu, J.; Fréchet, J. M. J.; Toney, M. F. Dependence of Regioregular Poly(3-Hexylthiophene) Film Morphology and Field-Effect Mobility on Molecular Weight. *Macromolecules* **2005**, *38*, 3312−3319.
(42) Verploegen, E.; Mondal, R.; Bettinger, C. J.; Sok, S.; Toney, M. F.; Bao, Z. Effects of Thermal Annealing upon the Morphology of Polymer−Fullerene Blends. *Adv. Funct. Mater.* **2010**, *20*, 3519−3529.
(43) Zhao, Y.; Zhao, X.; Roders, M.; Qu, G.; Diao, Y.; Ayzner, A. L.; Mei, J. Complementary Semiconducting Polymer Blends for Efficient Charge Transport. *Chem. Mater.* **2015**, *27*, 7164−7170.
(44) Balar, N.; O'Connor, B. T. Correlating Crack Onset Strain and Cohesive Fracture Energy in Polymer Semiconductor Films. *Macromolecules* **2017**, *50*, 8611−8618.
(45) Howard, J. B.; Ekiz, S.; Cuellar de Lucio, A. J.; Thompson, B. C. Investigation of Random Copolymer Analogues of a Semi-Random Conjugated Polymer Incorporating Thieno[3,4-B]Pyrazine. *Macromolecules* **2016**, *49*, 6360−6367.
(46) Kim, J.; Nizami, A.; Hwangbo, Y.; Jang, B.; Lee, H.; Woo, C.; Hyun, S.; Kim, T. Tensile Testing of Ultra-Thin Films on Water Surface. *Nat. Commun.* **2013**, *4*, 2520.
(47) Rodriquez, D.; Kim, J.; Root, S. E.; Fei, Z.; Boufflet, P.; Heeney, M.; Kim, T.; Lipomi, D. J. Comparison of Methods for Determining the Mechanical Properties of Semiconducting Polymer Films for Stretchable Electronics. *ACS Appl. Mater. Interfaces* **2017**, *9*, 8855−8862.
(48) Lipomi, D. J. Stretchable Figures of Merit in Deformable Electronics. *Adv. Mater.* **2016**, *28*, 4180−4183.
(49) Bruner, C.; Dauskardt, R. Role of Molecular Weight on the Mechanical Device Properties of Organic Polymer Solar Cells. *Macromolecules* **2014**, *47*, 1117−1121.

DOI: 10.1021/acsami.8b10608
ACS Appl. Mater. Interfaces 2018, 10, 32426−32434